An underwater stereo-camera trap

Article *in* Methods in Oceanography · December 2014

DOI: 10.1016/j.mio.2015.01.003

Christopher N. Rooper
National Oceanic and Atmospheric Administration

Methods in Oceanography 11 (2014) 1–12

Contents lists available at ScienceDirect

Methods in Oceanography

journal homepage: www.elsevier.com/locate/mio

Full length article

An underwater stereo-camera trap

Kresimir Williams *, Alex De Robertis, Zachary Berkowitz, Chris Rooper, Rick Towler

Alaska Fisheries Science Center, National Marine Fisheries Service NOAA, 7600 Sand Point Way NE, Seattle, WA, United States

ARTICLE INFO

Article history:
Received 30 October 2014
Received in revised form
6 January 2015
Accepted 20 January 2015

Keywords:
Underwater camera
Stereo-camera
Fish behavior

ABSTRACT

This paper describes the design and deployment of a new type of underwater stereo camera capable of triggering when animals are present in the field of view. Unobtrusive evaluation of the camera view field for potential targets is achieved using far-red illumination invisible to most fishes. The triggered camera (TrigCam) system is designed to be low cost by incorporating off-the-shelf commercial camera and computer components. It also incorporates several novel software and hardware developments such as the Cannon Hackers Development Kit which provides a high degree of control over the cameras, and a Raspberry Pi computer-on-board module for low-power, cost-efficient computing. The innovative triggering algorithm for fine control of the size and intensity of targets necessary to trigger an image is described in detail. Stereo image analysis provides estimates of fish size, position, and orientation to provide quantitative data from images. Test field deployments demonstrate operational capacity and illustrate potential applications for sampling marine organisms through example descriptions of analytical methods, including the trigger process and stereo image analysis. The TrigCam is intended to be an open source project to encourage continued development within the marine research community, with design information available through internet posts.

Published by Elsevier B.V.

* Corresponding author.
E-mail address: Kresimir.Williams@noaa.gov (K. Williams).

http://dx.doi.org/10.1016/j.mio.2015.01.003
2211-1220/Published by Elsevier B.V.

1. Introduction

Triggered autonomous cameras (*i.e*. camera traps) have long been used in terrestrial systems, but the technology has not been widely applied underwater (but see Jaffe et al., 1998). These instruments have been highly successful in studies where estimates of abundance or behavior are required without an observer effect. A relatively unobtrusive measurement device is highly desirable for marine studies, as different species and size classes of animals often have different probabilities of being detected by the observation platform due to behavior, resulting in a major source of uncertainty in animal abundance estimates (Fernö and Olsen, 1994). Here, we report on the construction of a new low-cost, minimally-invasive, motion-triggered underwater stereo camera system for underwater use.

Land-based camera traps have been used to measure the abundance (Karanth, 1995; Silver et al., 2004), species diversity (O'Brien et al., 2010), and behavior (Bridges et al., 2004; Maffei et al., 2005) of terrestrial species. Camera traps have been highly useful for counting cryptic, rare or shy species and for observing natural behaviors of animals without an observer effect. This has allowed researchers to estimate population numbers for species that are rare and difficult to assess via standard survey methods, such as endangered tigers in India (Karanth, 1995) and jaguars in the Amazon (Silver et al., 2004). Natural animal behaviors without an observer effect can be recorded using triggered cameras, and because of their portability and relatively low cost, more samples can potentially be collected with multiple triggered cameras. This approach can be much more cost effective relative to typical image based surveys such as autonomous underwater vehicles (AUV's) or remotely operated vehicles (ROV's) which are generally more complicated, requiring a field support team. The advantages of triggered cameras in estimating population abundance for rare species and observing natural behavior is directly relevant to multiple marine research themes. The types of data that can be extracted from triggered images include animal presence, location, density, habitat association, diurnal behavior patterns, and with the use of stereo cameras, animal size, position and orientation in the camera field of view.

It is important to minimize the stimuli produced by optical instruments used in visual surveys of fish populations, because the resulting abundance estimates can be strongly influenced by species- and size-specific fish behavior, such as avoidance. Fish avoidance or attraction to sampling vessels (De Robertis and Handegard, 2012) or submersible vehicles (Stoner et al., 2008) used to conduct optical surveys can bias density estimates (e.g. Koslow et al., 1995, Yoklavich et al., 2007 and O'Connell and Carlile, 1993). In most deep water marine environments, artificial lighting is necessary for optical surveys, and the reactions of fish to the intensity and type of lighting is poorly understood. In addition, there are reactions to the optical platform itself, especially for moving platforms such as remotely operated vehicles (ROV's) and drop cameras. For example, rockfish (*Sebastes* spp.) often have been suspected or observed to have an escape response to underwater vehicles (Krieger and Ito, 1999; Stoner et al., 2008; Ryer et al., 2009; Rooper et al., submitted for publication). This response may be species- and/or size-specific, in that some rockfish species may dive to the seafloor in the presence of an underwater vehicle, while others may react less (Rooper et al., submitted for publication). An escape response may be more prevalent in smaller size classes or species, where the risk of predation is greater. In addition to concerns related to surveys, other aspects of fish behavior are important, such as species-specific diel migrations, associations of fish with particular habitat types, or behaviors that influence the vulnerability of fishes to bottom trawls (such as fish hiding in interstitial spaces). These survey uncertainties would be reduced by the ability to observe species over longer time periods in a more "undisturbed" setting, where the observation platform is not influencing the behavior of the subjects.

The goal of this project was to develop a new class of underwater camera systems that leverage recent developments in off-the shelf consumer-grade components to construct a low-cost, motion-triggered, underwater, stereo camera trap (TrigCam). We designed and constructed the TrigCam with the goals that it would (1) minimize the behavioral reactions of fishes to artificial illumination, (2) allow for measurement of fish length and 3-dimensional spatial position and orientation using stereo optics, and (3) allow for observations at up to 300 m depth over long time periods (up to 24 h). Given that optical imaging has a relatively small sampling volume underwater due to absorption and scat-

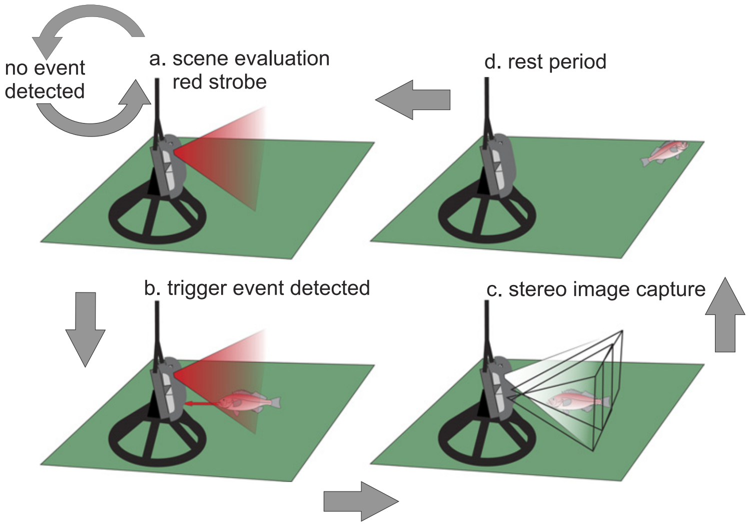

Fig. 1. Schematic showing the steps in TrigCam operation. Red illumination is used to detect the presence of a target (a, b) which is used to trigger the acquisition of a high-resolution image pair under white illumination (c), after which the fish reaction is not relevant and a rest period takes place before resumption of sampling (d). Red illumination is used to monitor for the presence of a target in the field of view to minimize reactions of animals near the camera. White illumination is used to "capture" a target, resulting in a high-resolution full color stereo image. (For interpretation of the references to color in this figure legend, the reader is referred to the web version of this article.)

tering of light, the intention was to keep costs low so that multiple systems can be deployed simultaneously to increase data density and make best use of vessel time in the field.

2. Materials and methods

Overview

Eight TrigCam units were built using consumer point and shoot cameras and custom low-cost electronics. The most innovative aspect of the TrigCams is the triggering mechanism. The purpose of the triggering mechanism (as in any photo trap) is to unobtrusively detect the subject prior to firing artificial lighting. Triggering is based on illumination from a far red (660 nm) light emitting diode (LED) array. In most deepwater (100 + m) fish species, sensitivity is minimal in red light, as this wavelength is not present in their habitat (Raymond and Widder, 2007; Brill et al., 2008). The presence of the trigger light should therefore be relatively unobtrusive to the fish and should not cause changes in behavior due to the presence of the light. The image space is monitored, and when a fish enters the image space, a white strobe light is triggered to provide high-quality illumination of a high-resolution pair of images (Fig. 1).

2.1. System description

The TrigCam consists of a camera housing, a strobe light, and a battery in separate underwater housings (Fig. 2). The main housing contains two Canon Powershot 300 HS point and shoot cameras, a single-board ARM (ARM Holdings PLC, Cambridge, UK) system-on-chip computer (Raspberry Pi, Raspberry Pi Foundation, Cambridgeshire, UK), and a custom circuit for power management and timing control of strobe pulses. The power board also contains a clock and small button battery, as the Raspberry Pi lacks a real time clock and has to rely on outside connectivity for this information. The housing was manufactured from 51 mm (2″) thick acetal plastic plate by milling out voids for the components and covering these with an o-ring sealed 19 mm (0.75″) acetal back plate. Images were taken through custom manufactured 80 mm radius acrylic partial domes. Domed viewports allowed

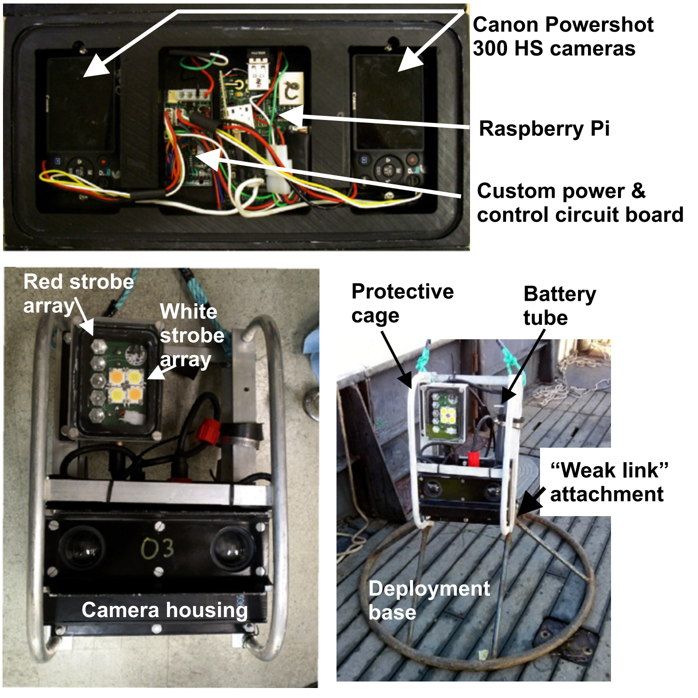

Fig. 2. Triggercam components. Upper panel shows camera housing with two Canon® 300 HS Powershot point-and-shoot cameras, a Raspberry Pi® system-on-chip computer, and a custom circuit board for power management and timing control of strobes. The camera housing and the strobe housing, which contains the red and white LED arrays, fit into a protective cage (lower left panel). This cage is mounted on a deployment base using a break-away link in case the unit gets trapped on the seafloor (lower right panel). (For interpretation of the references to color in this figure legend, the reader is referred to the web version of this article.)

wider view angles to be achieved, and minimized radial distortion caused by light refraction through flat viewports. The strobe housing was similarly manufactured from 51 mm acetal plastic, using a flat acrylic 19 mm (0.75″) back plate to allow light transmission from the LED elements. The strobe unit consisted of a vertically oriented five-element deep red LED array (LEDEngin®) discharging a narrow spectral band of light centered on 660 nm (±10 nm, Fig. 2). The vertically oriented red LED linear array with reflector cones and angular deflectors produces a vertically extended light beam. This configuration ensures that targets are more evenly detected in the vertical plane and are more likely to be captured in both of the horizontally offset cameras. A secondary four element square array of white LED modules (Bridgelux®) provides wide angle strobed white light for even image exposures with a combination of two cool white units (color temperature of 5600 K) and two warm white units (3000 K). Red and white LED arrays were powered by separate TaskLED® drivers capable of high current output necessary for strobed operation. The system was powered by 24 V 4.5 Ah nickel metal-hydride batteries housed in a cylindrical poly-vinyl chloride (PVC) housing fabricated from standard 64 mm (2.5″) high pressure (schedule 80) pipe. All housings were pressure tested to a depth of 500 m.

The cameras were controlled by installing an alternative firmware (Canon Hackers Development Kit, CHDK), an open source software project. The CHDK firmware allowed control scripts to be run on the onboard single-board computer to set exposure parameters on the cameras and allowed the computer to acquire image data from the cameras. The cameras were powered on and triggered by hard-wiring the camera power and trigger switches directly to a Pic® microcontroller on the customized circuit board. True native camera flash synchronization was not possible with dual cameras, so synchronous paired images were captured using a single strobe pulse while the shutters on both cameras were open using an exposure setting of 0.167 s.

2.2. Deployment

The TrigCam housings were mounted inside a protective aluminum cage, which was in turn attached to a steel base (Fig. 2) with a weak link that would allow the camera to be recovered if the base became entangled along the sea floor, in a fashion similar to that of Hannah and Blume (2012). Total unit weight in air was approximately 35 kg, with the camera components and aluminum cage weighing 12 kg. The system was rigged using a combination of 50 m of 9.5 mm floating line attached to the cage and 50 m of 9.5 mm sinking line connected to buoys at the surface to prevent entanglement both on the seafloor and at the deployment vessel. A pressure-tolerant float was attached approximately 3 m from the enclosure to ensure that the line remained clear of the camera gear. The buoy rig consisted of an inflatable buoy (of 30 kg buoyancy) followed by a pair of trailing floats at a distance of 10 m allowing efficient retrieval using a grappling hook.

Upon recovery of the TrigCams, the data collected during a deployment were transferred to a computer over a Wi-Fi link. The range of wireless communications (WiFi) was substantially enhanced by using plastic housings. This is important because stereo-calibrated camera systems remain useful as long as the camera geometry (i.e. inter-camera position) is stable, and not having to handle the cameras to remove images minimizes the potential for changes in position of cameras in housings (Williams et al., 2010).

2.3. Method of operation

Triggered images are captured by periodically evaluating the view field of a single camera and triggering the acquisition of a stereo-image pair when sufficient change has been detected. The camera system is controlled by a script written in the Python computer language which is executed on the single-board computer. The script contains commands to turn the cameras on, and to set exposure, gain (ISO), image size, and focus on each camera. In addition, CHDK code provides a method to extract the "live view buffer", which is where the camera stores data that is typically displayed continuously on the back screen of the camera. This reduced resolution image (740×280) is intensified by binning (adding up pixels) to form an 80×80 grid, which constitutes the trigger evaluation image (TEI). Binning greatly increases the sensitivity of image sensor, which is necessary because the use of far red lighting for illumination is very inefficient due to high absorption of this light frequency in water. Image binning also reduces the high level of noise due to the high gain settings on the camera for low light conditions, and reduces the transfer time for the data from the camera to the computer, resulting in decreased time intervals necessary between sequential trigger evaluation events. The red LED strobe is discharged as the TEI is captured, which requires precise timing between the strobe trigger and reading of the live view buffer.

After obtaining a TEI from the camera, a trigger detection algorithm running on the single board computer determines if an animal is present in the field of view. The trigger process is illustrated graphically in Fig. 3. The first step is to compute the absolute difference between the previous TEI and the current one (Fig. 3(a)–(c)), and apply a primary noise threshold (Fig. 3(d)). This step results in a binary 80×80 matrix. This matrix is then further binned into a 10×10 matrix (Fig. 3(e)), with each cell value indicating the total number of positive pixels in the corresponding 8×8 sub-square from the binary 80×80 matrix (maximum value $= 64$). A second threshold is applied to identify high value cells, which indicate the likelihood that an object is present. This approach allows the size and intensity of the target to be separately addressed with the two thresholds. A minimum and maximum target size is specified in number of 10×10 matrix cells above the second threshold. Occasional misalignments of the red strobe timing and TEI capture result in "level" shifts where the intensity of the image changes by a constant amount across the entire field of view. Setting a maximum target size to $< 1/4$ of the total number of matrix cells ($10 \times 10 = 100$) prevents a false trigger from occurring under these circumstances. Finally, portions of the 10×10 matrix can be ignored for triggering purposes. For example, the outer matrix edge cells can be ignored, preventing triggers from targets on the edge of the visual field that are not likely to be seen in both images of the stereo-pair. The TEI images are stored on the computer for review, allowing post-processing of the TEI images to fine tune the triggering algorithm for subsequent deployments.

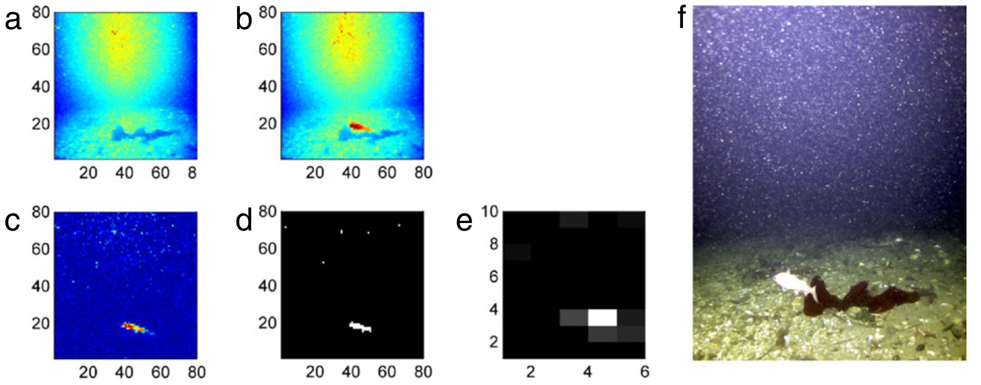

Fig. 3. Trigger evaluation process for the TrigCam. Panels a and b represent 80 × 80 trigger evaluation images taken 2 s apart. The difference image (c) shows the absolute change from image a to b with the fish target clearly seen in the lower portion and noise also visible in the upper portion. A threshold is applied, resulting in the binary image d, which is then aggregated into a 10 × 6 grid (e) where each cell represents the number of pixels above threshold in image d. A second threshold finds one cell in the binary matrix e to meet criteria for a trigger, resulting in firing of the cameras and strobe to obtain image f (right camera image shown). (For interpretation of the references to color in this figure legend, the reader is referred to the web version of this article.)

If the trigger evaluation indicates a suitable target was detected, the cameras are triggered resulting in high resolution (12 Mp) color synchronous image pairs (Fig. 3(f)). After a shot is taken, the system can be set to wait a specific interval of time to allow any fish responses to the white strobe to dissipate before trigger evaluation resumes (in our field tests, a 5 min wait time was used). Trigger evaluation ends when one of the following conditions is met: the total number of shots specified is taken, the specified deployment time is reached, or battery voltage drops below a specified threshold. The shutdown process includes copying the images from the camera SD cards to the single-board computer so they can be easily downloaded along with other deployment data, such as a system log file which contains operational details for each deployment to aid in troubleshooting.

2.4. Stereo analysis

To compute range information for simultaneously captured image pairs, the cameras were calibrated following methods described in Williams et al. (2010) using the Matlab Camera Calibration Toolbox (Bouguet, 2008). The calibration procedure corrects for distortion of the images due to the lens and viewport optics, as well as solving for the epipolar geometry between the two cameras. Once calibrated, three dimensional coordinates can be determined for any corresponding point that is identified in the stereo-image pair using a stereo-triangulation function supplied with the calibration toolbox. The calibration parameters derived by this process remain useful as long as the cameras do not move relative to each other, meaning the cameras should not be removed from the housings during field operations.

3. Results and discussion

3.1. Test deployments

A series of system tests were conducted at the Friday Harbor Laboratory, University of Washington, Friday Harbor, WA, in November 2013. The camera system was deployed from a research vessel in several locations within 20 km of the laboratory, and at the laboratory dock overnight. The unit was lowered onto the seafloor at desired locations, and retrieved using a standard commercial hydraulic pot puller, with both deployment and retrieval each requiring approximately 15 min at depths of up to 80 m. The battery pack used here provided a maximum system run time of 12 h with TEI images

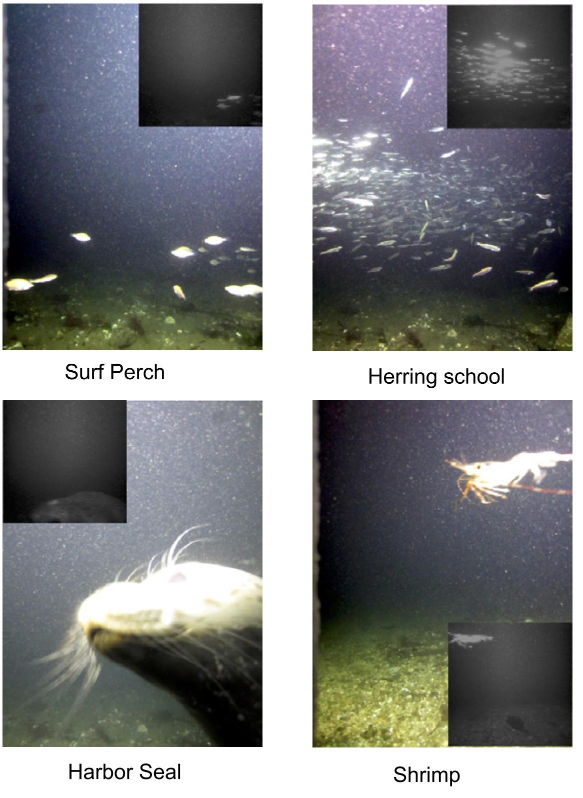

Fig. 4. Examples of targets captured by the TrigCam during test trials near Friday Harbor, Washington. The inset grayscale images show the trigger evaluation images associated with the target detection event. Only one of the images in the pair is shown.

collected every 2 s. Fig. 4 shows examples of animals captured by the TrigCam during these test deployments.

3.2. Reducing sampling impact with red light

Red and infrared light is widely used in terrestrial applications to unobtrusively illuminate security cameras and in trail cameras used to image wildlife (Silver et al., 2004). In the marine environment, infrared light is absorbed rapidly with range, and far red light is more practical. Many marine fishes and crustaceans have limited sensitivity to wavelengths greater than 620 nm (e.g. Boden and Kampa, 1965 and Brill et al., 2008). Thus red illumination has been used to minimize behavioral reactions to camera illumination in many marine applications (e.g. Jaffe et al., 1998 and Jury et al., 2001). The use of red lights have been shown to minimize the behavioral response of fishes to artificial illumination (Widder et al., 2005; Raymond and Widder, 2007). This is corroborated by a recent study, where abundances of juvenile rockfish from a towed camera system were 3.5 times higher when illuminated by red strobes compared to white lights, with the discrepancy decreasing with range (Rooper et al., submitted for publication).

Although red light is likely to be less stimulating than light at shorter wavelengths and is not absorbed by seawater as strongly as infrared light, it is still less effective for getting sufficiently exposed high-resolution images without specialized high cost camera equipment. In the TrigCam application, a red strobe is used to collect the low-resolution, high-sensitivity TEI images used to monitor the field of view for targets. The goal is to minimize disturbance, and white light, which is more likely to alter

Table 1
Performance comparison of an intervalometer and triggered camera systems. Images taken were 6 Mp, 24-bit color format (2112 × 2816 pixels), compressed using the jpeg method to produce a ∼1–1.5 MB image file. Approximate run time in this example is 5.3 h. Data are based on a single TrigCam test deployment.

Intervalometer system				
	Shot interval (s)	Total shots taken	Targets captured	Data Collected (GB)
	2	9584	18	24.1
	4	4792	9	12.04
	10	1917	3.6	4.82
	20	959	1.8	2.42
Triggered system	–	18	18	0.13[a]

[a] Includes 9584 80 × 80 pixel trigger evaluation images, 5–6 kb each.

the behavior of fishes, is only used to provide high-quality illumination to expose a triggered stereo image. It is likely that the white strobe will elicit a behavioral reaction, but by that point, the image has already been collected. This is very similar in design to the broadly used terrestrial trail cams that use an infra-red beam to trigger acquisition of wildlife images (e.g. Karanth, 1995 and Bridges et al., 2004). It is also possible that the TrigCam can modify animal behavior by the presence of the system itself, similar to a fish aggregating device (FAD) effect. Future developments to minimize physical size of the camera system would further remove these kinds of observational effects.

3.3. *Efficiency vs. time lapse*

A common method of optical sampling for extended periods of time is time-lapse recording, with instruments equipped with an intervalometer capable of triggering images or taking video segments at set time intervals. The efficacy of this approach can be compared with a triggered system by examining the stored TEI's from a test deployment. In most prolonged un-baited camera deployments in low fish density locations, few if any targets of interest are captured by the camera. This means that images taken on a timed basis will produce a high proportion of empty images. In addition, many camera systems require additional light, which if operated on a timed cycle can cause avoidance reactions by the animals. TrigCam also collects images at set intervals, but the key difference is that the TrigCam's TEI's are low bandwidth and therefore consume less memory resources than a comparable system only equipped to take high resolution images. The TEI's do not need to be stored, but they represent a meaningful method of ensuring the system is performing as expected. While a time lapse system could also selectively retain images based on content, TrigCams offer additional advantages over this approach by collecting two "tiers" of images. First is that the computing power necessary to compare image frames to detect an event is small using TEI's due to their low resolution. A system that had to evaluate differences in 6 Mp images would require more computing power or time to process inter-frame differences, making it more difficult to make use of low-cost, low power consumption ARM-based processors such as Raspberry Pi. Second, and more important, is the TrigCam approach of using a less obtrusive red light trigger to detect targets as opposed to a time lapse system. The red light trigger is critical for optimized sampling of deep water marine environments where ambient light is insufficient for "un-aided" motion based triggering. TEI's are insufficient to properly expose images required for analysis as color is often required for identifying species, and the high level of binning necessary for getting appropriate exposures results in low resolution images with insufficient detail. However, even at reduced resolution, the TEI's are sufficient to detect the presence of targets. The second tier full resolution images captured by the TrigCam allow for appropriately illuminated images that can be used to identify animals over a range of sizes and distances from the camera. Full spectrum (i.e. white light) illumination can cause reactions in fish after the shot is taken. However, the moment captured by the image, as with terrestrial camera traps, can be considered to be a relatively unbiased observation. A performance comparison between the TrigCam and a relatively simple time lapse system that stores all images is given in Table 1.

TrigCam approach also improves sampling efficiency by being able to test for the presence of targets at fairly rapid intervals. To achieve a similar sampling density using a simple time lapse system,

Table 2
A comparison of triggering algorithm performance given three threshold levels. Lower thresholds result in a higher false trigger rate, but enable smaller, lower contrast targets to be captured. The mean target intensity represents the average luminosity of the pixel area occupied by the target relative to the previous frame.

Threshold level	Primary threshold	Secondary threshold	Targets detected	False target rate (%)	Mean target size (pix)	Mean target intensity
High	50	15	18	0	13.5	80.2
Mid	25	10	87	28	5.0	40.5
Low	18	10	159	50	2.5	29.0

where each sampling event had to be collected at full resolution regardless of the presence of targets, much more data have to be stored, transferred, and analyzed, reducing efficiency. A comparison in memory requirements between time-lapse and triggered approaches is given in Table 1. The trigger approach is more complex than using time-lapse methods, but the increased performance and efficiency may be justified when data collection opportunities are limited. For many marine researchers, the overall increase in sampling efficiency as approximated by number of useful images acquired per unit time may be of greatest importance when sampling the marine environment in applications that rely on expensive vessel time. In addition, restricting an analysis to only images that contain targets reduces the time required for analysis by removing the "search" time and transferring and archiving the image data.

3.4. *Trigger performance*

Test deployments were evaluated for trigger performance, including false triggers and missed targets. Fig. 5 demonstrates the utility of retaining the TEI's for post analysis, as the data can be "replayed" with different threshold settings to investigate triggering efficiency. Three levels of thresholds were analyzed resulting in different levels of success and selecting for different target sizes and target intensities (Table 2). The timeline of trigger events shows that in this example they are clustered, meaning fish appear and remain in the view for limited intervals, often followed by long intervals without any activity in front of the camera. In addition, intervals of high TEI "noise" due to suspended particles in the water or changing turbidity can cause significant false triggers with low threshold settings (e.g. between interval between hours 7 and 8). Threshold settings have a strong influence on the data collected and have to be chosen with consideration to collection objectives. For example, if smaller, less intense targets need to be captured, a low threshold may be necessary, and a high level of false triggers is unavoidable. However, if only larger intense targets are sought, false trigger rates can be virtually eliminated using high thresholds.

3.5. *Stereo-analysis*

Following stereo-calibration, several additional metrics that relate to estimating fish behavior could be determined. In an example analysis (Fig. 6), individual fish were analyzed by extracting the pixel coordinates of the snout and tail in both the left and right camera images.

These points were then converted to three-dimensional coordinates using stereo triangulation, and the length of the fish was estimated using Cartesian distance between the head and tail points. In addition, points along the seafloor were identified and triangulated and used to interpolate a surface representing the seafloor. The types of information that this analysis yielded such as fish length, nearest-neighbor distance, relative orientations, and height off bottom could be used to study in situ animal behavior in an undisturbed state, which is difficult to achieve by other means.

3.6. *Conclusions and potential applications in marine environments*

In the test deployments, TrigCam performed well, allowing efficient, unobtrusive optical sampling of the marine environment over extended time scales. The use of stereo-cameras greatly increases the amount of quantitative data that can be extracted from images, enabling researchers to address a variety of hypotheses. While the system is relatively complex, the use of commercial off-the-shelf

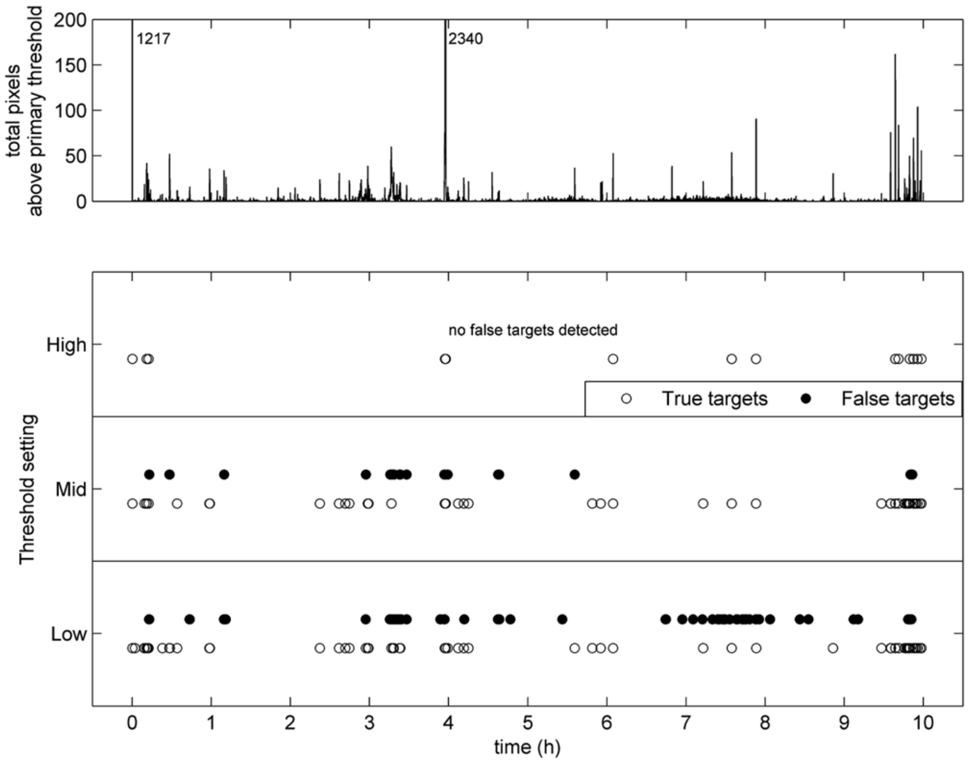

Fig. 5. Example of trigger operation using the TrigCam system. The upper panel shows the magnitude of the frame-to-frame change as the number of pixels that exceed the primary threshold applied to the absolute difference image. The lower panels show the time line of trigger occurrences at three different threshold settings. Further details from this comparison are given in Table 2.

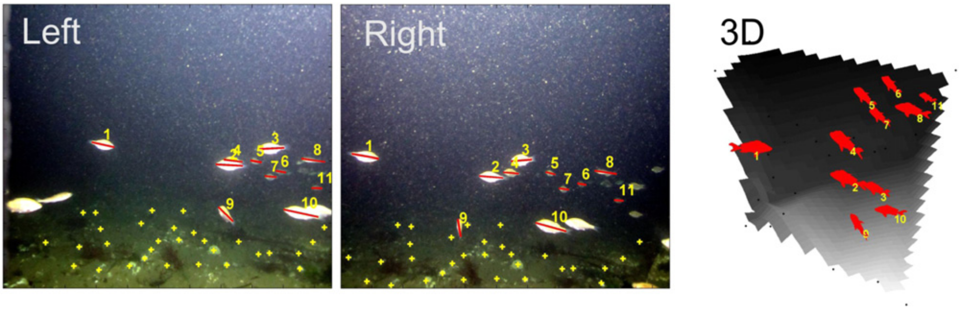

Fig. 6. An example of a stereo image analysis using TrigCam still images. The left and right images show the user-determined corresponding locations of fish snout and tail (red lines), as well as corresponding points on the seafloor (yellow crosses). This information is then used to reproduce a 3 dimensional representation on the far right with fish models showing position, size, and orientation of fish targets and a surface fit to the seafloor points. Only those fish imaged in both cameras are displayed in the model. (For interpretation of the references to color in this figure legend, the reader is referred to the web version of this article.)

equipment and low-cost housings makes the units affordable and reduces the financial consequences of loss, which is a concern for all autonomous instruments. Lower unit cost also opens up the simultaneous deployment of many units, which is necessary for some studies to counteract low sampling volumes inherent in optical sampling systems, and potentially a low encounter rate with rare organisms.

Table 3
Current (2014) TrigCam component costs. The labor costs for fabrication of housings, assembly of components, and welding of protective cage are not included in this estimate.

Item	Description/source	Quantity	Amount (US $)
Cameras	Canon powershot 300 HS	2	200
Housings (materials only)	2″ Delrin® plate	1	150
Underwater cables	SubConn	1	287
Acrylic domes	Global precision optics	2	70
Raspberry Pi	Raspberry Pi foundation	1	35
Batteries	NiMH 12 V 4500 mAh/BatterySpace	2	54
Custom power board (components only)	n/a	1	25
Strobes (components only)	n/a	1	125
Aluminum cage (materials only)	n/a	1	35
Miscellaneous electronic components	n/a	1	50
Sacrificial steel base	n/a	1	150
Deployment rig (line, buoys, hardware)	n/a	1	250
Total			1755

Approximate estimates of current (2014) component costs are given in Table 3. These are underestimates of the total cost as the labor for machining and assembly are not included. In comparison with commercially available underwater camera systems rated for depths of up to 500 m, the component costs are substantially lower. The authors are developing a web page containing information on system design, such as housing drawings and trigger operation software. With this posting we hope to foster interest and possibly engage other marine research groups to build their own units and possibly continue development of this type of device for public benefit. To promote the usability and continued developments of this project, we have used open source software platforms wherever possible. Please contact authors for more information on this development.

The TrigCam design described here could be easily modified for deployment times of up to 24 h or more with larger battery packs, making it suitable for deployment on a stationary base or mooring. This type of sampling approach promises to maximize the use of vessel time as units can be sequentially deployed and then retrieved. Potential research questions that could be studied using the TrigCam include diel patterns in fish behavior, encounter of rare animals occurring in low density, detection of fish in areas poorly sampled by other devices, and general descriptions of fish behavior such as intra-fish distance and orientation in schools and positions relative to the seafloor or other features.

Acknowledgments

The development and testing of the TrigCams was funded by NOAA's Advanced Sampling Technology Working Group. The research and development presented here greatly benefited from the support of Chris Wilson and David King from the Alaska Fisheries Science Center. We also want to acknowledge David Duggins, Dennis Willows, Kristy Kull (FHL) and James Fahlbusch of UW-Friday Harbor Laboratory for their assistance during field tests.

The findings and conclusions in the paper are those of the authors and do not necessarily represent the views of the National Marine Fishery Service, NOAA. Reference to trade names does not imply endorsement by the National Marine Fisheries Service, NOAA.

References

Boden, B.P., Kampa, E.M., 1965. An aspect of euphausiid ecology revealed by echo sounding in a fjord. Crustaceana 9, 155–173.
Bouguet, J.Y., 2008. Camera calibration toolbox for MATLAB (online). (Available from http://vision.caltech.edu/bouguetj/calib_doc/index.html (accessed September 2008)).
Bridges, A.S., Vaughan, M.R., Klenzendorf, S., 2004. Seasonal variation in American black bear *Ursus americanus* activity patterns: quantification via remote photography. Wildl. Biol. 10, 277–284.
Brill, R., Magel, C., Davis, M., Hannah, R., Rankin, P., 2008. Effects of rapid decompression and exposure to bright light on visual function in *Sebastes melanops* and *Hippoglossus stenolepis*. Fish. Bull. 106, 427–437.
De Robertis, A., Handegard, N.O., 2012. Fish avoidance of research vessels and the efficacy of noise reduced vessels: a review. ICES J. Mar. Sci. 70, 34–35.

Fernö, A., Olsen, S. (Eds.), 1994. Marine Fish Behaviour Related to Capture and Abundance Estimation. In: Fishing News Books, Blackwell Science Ltd., Oxford, p. 211.
Hannah, R.W., Blume, M.T., 2012. Tests of an experimental unbaited video lander as a marine fish survey tool for high-relief deepwater rocky reefs. J. Exp. Mar. Biol. Ecol. 430–431, 1–9.
Jaffe, J.S., Ohman, M.D., De Robertis, A., 1998. OASIS in the sea: measurement of the acoustic reflectivity of zooplankton with concurrent optical imaging. Deep-Sea Res. 45, 1239–1253.
Jury, S.H., Howell, H., O'Grady, D.F., Watson, W.H., 2001. Lobster trap video: in situ video surveillance of the behaviour of *Homarus americanus* in and around traps. Mar. Freshwater Res. 52, 1128–1132.
Karanth, K.U., 1995. Estimating tiger (*Panthera tigris*) populations from camera-trap data using capture–recapture models. Biol. Conserv. 71, 333–338.
Koslow, J.A., Kloser, R., Stanley, C.A., 1995. Avoidance of a camera system by a deepwater fish, the orange roughy (*Hoplostethus atlanticus*). Deep-Sea Res. 42, 233–244.
Krieger, K.J., Ito, D.H., 1999. Distribution and abundance of shortraker rockfish, *Sebastes borealis*, and rougheye rockfish, *S. aleutianus*, determined from a manned submersible. Fish. Bull. 97, 264–272.
Maffei, L., Noss, A.J., Cuellar, E., Rumiz, D.I., 2005. Ocelot (*Felis pardalis*) population densities, activity and ranging behaviour in the dry forests of eastern Bolivia: data from camera trapping. J. Trop. Ecol. 21, 349–353.
O'Brien, T.G., Kinnaird, M.F., Wibisono, H.T., 2010. Estimation of species richness of large vertebrates using camera traps: an examples from an Indonesian rainforest. In: O'Connell, A.F., Nichols, J.D., Karanth, K.U. (Eds.), Camera Traps in Animal Ecology: Methods and Analyses. Springer Verlag, Tokyo.
O'Connell, V.M., Carlile, D.W., 1993. Habitat-specific density of adult yelloweye rockfish *Sebastes ruberrimus* in the eastern Gulf of Alaska. Fish. Bull. 91, 304–309.
Raymond, E.H., Widder, E.A., 2007. Behavioral responses of two deep-sea fish species to red, far-red, and white light. Mar. Ecol. Prog. Ser. 350, 291–298.
Rooper, C.N., Williams, K., De Robertis, A., Tuttle, V.J., Effect of underwater lighting on observations of density and behavior of rockfish during camera transects (submitted for publication).
Ryer, C.H., Stoner, A.W., Iseri, P.J., Spencer, M.L., 2009. Effects of simulated underwater vehicle lighting on fish behavior. Mar. Ecol. Prog. Ser. 391, 97–106.
Silver, S.C., Ostro, L.E.T., Marsh, L.K., Maffei, L., Noss, A.J., Kelly, M.J., Wallace, R.B., et al., 2004. The use of camera traps for estimating jaguar *Panthera onca* abundance and density using capture/recapture analysis. Oryx 38, 148–154.
Stoner, A.W., Ryer, C.H., Parker, S.J., Auster, P.J., Wakefield, W.W., 2008. Evaluating the role of fish behavior in surveys conducted with underwater vehicles. Can. J. Fish. Aquat. Sci. 65, 1230–1243.
Widder, E.A., Robison, B.H., Reisenbichler, K.R., Haddock, S.H.D., 2005. Using red light for in situ observations of deep-sea fishes. Deep-Sea Res. I 52, 2077–2085.
Williams, K., Rooper, C.N., Towler, R.H., 2010. Use of stereo camera systems for assessment of rockfish abundance in untrawlable areas and for recording pollock behavior during midwater trawls. Fish. Bull. 108, 352–362.
Yoklavich, M.M., Love, M.S., Forney, K.A., 2007. A fishery-independent assessment of an overfished rockfish stock, cowcod (*Sebastes levis*), using direct observations from an occupied submersible. Can. J. Fish. Aquat. Sci. 64, 1795–1804.